. SCUOLA INTERNAZIONALE SUPERIORE DI STUDI AVANZATI

SISSA Digital Library

Interplay of charge and spin dynamics after an interaction quench in the Hubbard model

Original
Interplay of charge and spin dynamics after an interaction quench in the Hubbard model / Wysokiński, M.M., Fabrizio, M.. - In: PHYSICAL REVIEW. B. - ISSN 2469-9950. - 96:20(2017), pp. 1-5. [10.1103/PhysRevB.96.201115]

Availability:
This version is available at: 20.500.11767/72023 since: 2023-08-17T04:32:59Z

Publisher:

Published
DOI:10.1103/PhysRevB.96.201115

Terms of use:

Testo definito dall'ateneo relativo alle clausole di concessione d'uso

Publisher copyright
APS - American Physical Society

This version is available for education and non-commercial purposes.

note finali coverpage

(Article begins on next page)

09 September 2026

Interplay of charge and spin dynamics after an interaction quench in the Hubbard model

Marcin M. Wysokiński[1, 2, *] and Michele Fabrizio[1, †]

[1] *International School for Advanced Studies (SISSA), via Bonomea 265, IT-34136, Trieste, Italy*
[2] *Marian Smoluchowski Institute of Physics, Jagiellonian University, ulica prof. S. Łojasiewicza 11, PL-30-348 Kraków, Poland*

(Dated: November 7, 2017)

We investigate the unitary dynamics following a sudden increase $\Delta U > 0$ of repulsion in the paramagnetic sector of the half-filled Hubbard model on a Bethe lattice, by means of a variational approach that combines a Gutzwiller wavefunction with a partial Schrieffer-Wolff transformation, both defined through time-dependent variational parameters. Besides recovering at ΔU_c the known dynamical transition linked to the equilibrium Mott transition, we find pronounced dynamical anomaly at larger $\Delta U_* > \Delta U_c$ manifested in a singular behaviour of the long-time average of double occupancy. Although the real-time dynamics of the variational parameters at ΔU_* strongly resembles the one at ΔU_c, careful frequency spectrum analysis suggests a dynamical crossover, instead of a dynamical transition, separating regions of a different behaviour of the spin-exchange.

arXiv:1711.01840v1 [cond-mat.str-el] 6 Nov 2017

Pump-probe time-resolved spectroscopy is growing in importance as a tool for studying and manipulating correlated materials [1]. On one hand it gives access to new enlightening information about the dynamical properties of those materials, beyond reach of conventional spectroscopy. In addition, it provides a very efficient tool to drive phase transitions on ultra-short time scales, and concurrently investigate them in the time domain. There are cases where the photo-induced phases are actually those observed at thermal equilibrium upon heating, like for instance in photo-excited VO_2 [2]. This might be suggestive of a quasi-thermal pathway, though that is not generically the case, even in the same VO_2 [3]. Indeed, there are evidences of photo-induced hidden phases that are absent at equilibrium [4, 5], as well as of remarkable non-thermal transient properties [6, 7].

At first sight it might seem unsurprising to observe non-thermal behaviour in correlated electron systems, which are complex materials with several competing phases and many actors playing a role. In reality, even the simplest among all models of correlated electrons, i.e. the single-band Hubbard model where the complexity of real materials is reduced just to the competition between the on-site repulsion U and the nearest-neighbour hopping t, shows puzzling and still controversial non-thermal behaviour. In a seminal work [8], Eckstein, Kollar and Werner discovered by time-dependent dynamical mean-field theory (t-DMFT) that the unitary evolution of the half-filled Hubbard model in an infinitely coordinated Bethe lattice after a sudden increase of the repulsion U from the initial $U_0 = 0$ to a final $U_f > 0$ displays a sharp crossover at $U_f = U_c$, which, within the relatively-short numerically-affordable simulation times, resembles a genuine dynamical transition. Such an interpretation was however contrasted by the observation that, if one assumes thermalisation, the temperature that corresponds to the energy supplied by the quench $U = 0 \to U_c$ is well above the second-order critical endpoint of the Mott-transition line in the T vs. U equilibrium phase diagram [8]. The same dynamical crossover was later found, still in an infinitely coordinated lattice, by a variational approach based on a time-dependent Gutzwiller wavefunction [9, 10], which is not as rigorous as t-DMFT but allows simulating much longer times. In particular, by considering a linear ramp rather than a sudden quench, this crossover was shown [11] to be a genuine dynamical transition linked to the equilibrium Mott transition. The same conclusion has been recently drawn by the nonequilibrium self-energy functional theory [12], which is supposed to be more rigorous than the variational Gutzwiller approach, though not as much as t-DMFT. We emphasise that, should this dynamical anomaly be confirmed to correspond to a dynamical Mott transition, it would imply [8] that even the simplest single-band Hubbard model may display non-thermal behaviour, at least in lattices with infinite coordination number. However, there are evidences that the same occurs also when the coordination is finite [13, 14].

It is therefore worth proving or disproving the existence of this dynamical transition by other complementary techniques, looking forward to numerical developments that could allow t-DMFT to finally settle this issue. Here we make such an attempt by extending out of equilibrium the variational approach that we recently proposed [15], and which combines a Gutzwiller wavefunction with a partial Schrieffer-Wolff transformation, both defined now by time-dependent variational parameters. At equilibrium, this variational wavefunction provides a much better description of the Mott insulator than the simple Gutzwiller wavefunction, and it is therefore likely it may also describe more accurately the non-equilibrium dynamics.

We consider the half-filled single-band Hubbard model

on an infinitely coordinated Bethe lattice,

$$H(t) = -\frac{1}{\sqrt{z}} \sum_{<ij>} T_{\mathbf{ij}} + \frac{\mathrm{U}(t)}{2} \sum_{\mathbf{i}} \left(n_{\mathbf{i}\uparrow} + n_{\mathbf{i}\downarrow} - 1 \right)^2 , \quad (1)$$

where $z \to \infty$ is the coordination number, $\mathrm{U}(t)$ the time-dependent on-site repulsion, $\mathrm{U}(t<0) = \mathrm{U}_0$ and $\mathrm{U}(t \geq 0) = \mathrm{U}_f$, and $T_{\mathbf{ij}} \equiv \sum_\sigma (c^\dagger_{\mathbf{i}\sigma} c_{\mathbf{j}\sigma} + H.c.)$ the hopping operator on the bond $<ij>$ connecting the nearest-neighbour sites i and j.

The dynamics of the model is determined through the saddle point of the action

$$\mathcal{S} = \int dt \, \langle \Psi(t)| \, i \frac{d}{dt} - H(t) \, |\Psi(t)\rangle \, , \quad (2)$$

which provides the exact solution of the Schrödinger equation for unrestricted many-body wavefunctions $\Psi(t)$, or just a variational estimate of it in case $\Psi(t)$ varies within a subspace of the whole Hilbert space, which is what we shall do hereafter. In particular, we assume for $\Psi(t)$ the expression [15],

$$\big|\Psi(t)\big\rangle = \mathcal{U}(t) \, \mathcal{P}_G(t) \, \big|\psi_0(t)\big\rangle \, , \quad (3)$$

where $\psi_0(t)$ is a paramagnetic uniform Slater determinant, $\mathcal{U}(t)$ a unitary transformation, and finally $\mathcal{P}_G(t) \equiv \prod_{\mathbf{i}} \mathcal{P}_{\mathbf{i}}(t)$, with $\mathcal{P}_{\mathbf{i}}(t)$ a linear operator on the local Hilbert space [9]. In the presence of particle-hole symmetry and discarding spontaneous breakdown of spin $SU(2)$ symmetry, $\mathcal{P}_{\mathbf{i}}(t)$ can be generically written as

$$\mathcal{P}_{\mathbf{i}}(t) = \sqrt{2} \, \phi_{\mathbf{i}0}(t) \Big[\mathrm{P}_{\mathbf{i}}(0) + \mathrm{P}_{\mathbf{i}}(2) \Big] + \sqrt{2} \, \phi_{\mathbf{i}1}(t) \, \mathrm{P}_{\mathbf{i}}(1) \, , \quad (4)$$

where $\mathrm{P}_{\mathbf{i}}(n)$ is the projection operator at site i onto the configuration with n electrons, whereas $\phi_{\mathbf{i}n}(t)$ is a complex function of time [9]. In infinitely coordinated lattices the wavefunction $|\Psi(t)\rangle$ is normalised at any time if $|\phi_{\mathbf{i}0}(t)|^2 + |\phi_{\mathbf{i}1}(t)|^2 = 1$.

The time-dependent unitary transformation $\mathcal{U}(t)$ is of the Schrieffer–Wolff type [15–17], and it is parametrised by complex, time and bond dependent variational parameters $\epsilon_{\mathbf{ij}}(t)$:

$$\mathcal{U}(t) \equiv \mathrm{e}^{A(t)} \equiv \exp \left[\frac{1}{\sqrt{z}} \sum_{\langle \mathbf{ij} \rangle} \Big(\epsilon_{\mathbf{ij}}(t) \, \tilde{T}_{\mathbf{ij}} - \epsilon^*_{\mathbf{ij}}(t) \, \tilde{T}^\dagger_{\mathbf{ij}} \Big) \right] , \quad (5)$$

where

$$\begin{aligned} \tilde{T}_{\mathbf{ij}} &\equiv \Big(\mathrm{P}_{\mathbf{i}}(2)\mathrm{P}_{\mathbf{j}}(0) + \mathrm{P}_{\mathbf{i}}(0)\mathrm{P}_{\mathbf{j}}(2) \Big) \, T_{\mathbf{ij}} \, \Big(\mathrm{P}_{\mathbf{i}}(1)\mathrm{P}_{\mathbf{j}}(1) \Big) , \\ \tilde{T}^\dagger_{\mathbf{ij}} &\equiv \Big(\mathrm{P}_{\mathbf{i}}(1)\mathrm{P}_{\mathbf{j}}(1) \Big) \, T_{\mathbf{ij}} \, \Big(\mathrm{P}_{\mathbf{i}}(2)\mathrm{P}_{\mathbf{j}}(0) + \mathrm{P}_{\mathbf{i}}(0)\mathrm{P}_{\mathbf{j}}(2) \Big) , \end{aligned} \quad (6)$$

are the components of the hopping operator T_{ij} that couple the low-energy subspace of singly occupied sites i and j with the high-energy one where one site is empty and the other doubly occupied.

We determine $\psi_0(t)$, $\mathcal{P}_G(t)$ and $\mathcal{U}(t)$ through the saddle point of the action (2) with respect to all the variational parameters, handling $\mathcal{U}(t)$ by a series expansion

$$U^\dagger \mathcal{O} \, U = \mathcal{O} - [A, \mathcal{O}] + \frac{1}{2} \Big[A, [A, \mathcal{O}] \Big] + \dots \, , \quad (7)$$

up to the desired order. For instance

$$\begin{aligned} U^\dagger \, H \, U \simeq H + \frac{U}{\sqrt{z}} \sum_{\mathbf{ij}} \Big(\epsilon_{\mathbf{ij}} \, \tilde{T}_{\mathbf{ij}} + \epsilon^*_{\mathbf{ij}} \, \tilde{T}^\dagger_{\mathbf{ij}} \Big) \\ + \frac{1}{8z} \sum_{\mathbf{ij}} J_{\mathbf{ij}} \Big[\tilde{T}_{\mathbf{ij}} + \tilde{T}^\dagger_{\mathbf{ij}} \, , \, \tilde{T}_{\mathbf{ij}} - \tilde{T}^\dagger_{\mathbf{ij}} \Big] + H_{\mathcal{R}} \, , \end{aligned} \quad (8)$$

where,

$$J_{\mathbf{ij}} = 4 \left[\big(\epsilon_{\mathbf{ij}} + \epsilon^*_{\mathbf{ij}} \big) \, V - U \, \big| \epsilon_{\mathbf{ij}} \big|^2 \right] , \quad (9)$$

and higher order terms are stored together in $H_{\mathcal{R}}$. In the calculation below we stop the series expansion at the third order in power of ϵ, and consider all processes up to three neighbouring sites. We have tested such an approximation at equilibrium in comparison with exact DMFT results [18], and it provides a quite satisfactory description of metal and insulating phases for $\mathrm{U} \gtrsim \mathrm{U}_{\mathrm{Mott}}/2$, where $\mathrm{U}_{\mathrm{Mott}}$ is the equilibrium location of the Mott transition (cf. Supplemental Material, Sec.I [19]). Inclusion of higher orders systematically increases the accuracy and thus allows accessing also the weaker correlated regime [15]. However, for the sake of simplicity, we decided to stand to the above approximation, and consequently we just considered quantum quenches from a relatively correlated metal at $\mathrm{U}_0 > \mathrm{U}_{\mathrm{Mott}}/2$ to higher values of $\mathrm{U}_f > \mathrm{U}_0$.

With this prescription for handling the unitary operator $\mathcal{U}(t)$, the expectation values that define the action (2) can be explicitly evaluated when the coordination number $z \to \infty$, and can be formally written as

$$\begin{aligned} \langle \Psi | i \frac{d}{dt} | \Psi \rangle &= i \, \langle \psi_0 | \dot{\psi}_0 \rangle + i \sum_{\mathbf{i}} \Big(\phi^*_{\mathbf{i}1} \, \dot{\phi}_{\mathbf{i}1} + \phi^*_{\mathbf{i}0} \, \dot{\phi}_{\mathbf{i}0} \Big) \\ &\quad + i \, f \Big(\mathbf{v}, \dot{\epsilon}_{\mathbf{ij}}, \dot{\epsilon}^*_{\mathbf{ij}}, \psi_0, \psi^*_0 \Big) \, , \\ \langle \Psi | H | \Psi \rangle &= h \big(\mathbf{v}, \psi_0, \psi^*_0 \big) , \end{aligned} \quad (10)$$

where $\mathbf{v} = \{ \phi_{\mathbf{i}0}, \phi^*_{\mathbf{i}0}, \phi_{\mathbf{i}1}, \phi^*_{\mathbf{i}1}, \epsilon_{\mathbf{ij}}, \epsilon^*_{\mathbf{ij}} \}$. Being too lengthy, the actual expressions of the functions f and h are given in the Supplemental Material, Sec.II [19].

The saddle point equations that determine the evolution of the wavefunction can be readily obtained. Like in the time-dependent Gutzwiller approximation [9], the evolution of the Slater determinant $\psi_0(t)$ is trivially just the multiplication by a time dependent phase, so that, for instance, $\langle \psi_0(t) | \frac{1}{\sqrt{z}} \sum_{ij} T_{\mathbf{ij}} | \psi_0(t) \rangle = 8/3\pi \equiv T_0$ is time independent. In what follows, we shall use as energy unit $8T_0$, and define $u = \mathrm{U}/8T_0$. In these units,

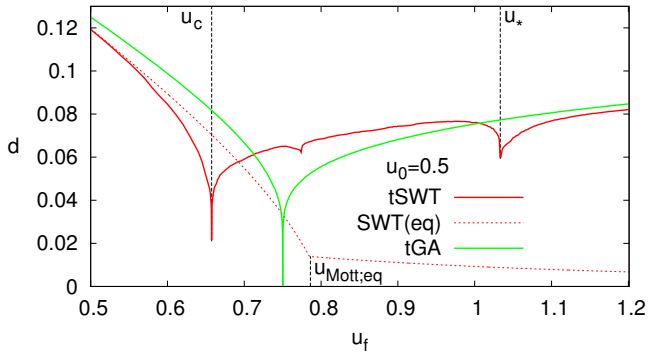

FIG. 1: Average double occupancy after the quench from the correlated metal at $u_0 = 0.5$. For the sake of completeness, we also show the equilibrium result (SWT) [15] as well as that obtained by the simpler Gutzwiller wavefunction (tGA) [9].

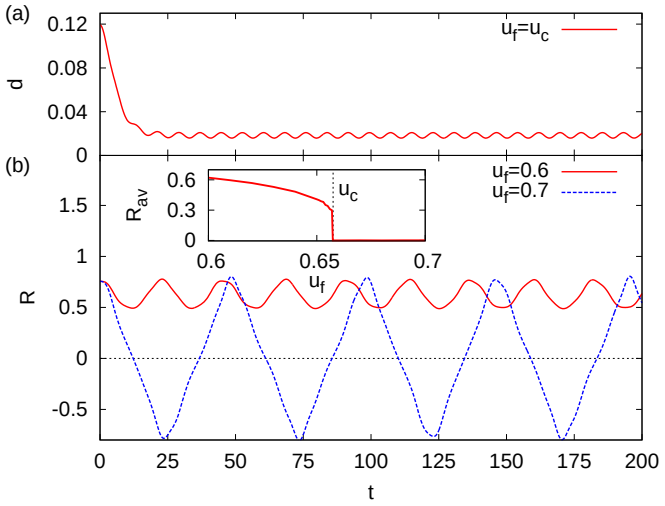

FIG. 2: Panel (a): time evolution of the double occupancy $d(t)$ at u_c. Panel (b): time evolution of $R(t)$ just before and after u_c, with its time average drawn in the inset. We note that indeed R has a critical behaviour at u_c.

the initial state is always prepared at $u_0 = 0.5$ and then instantly quenched to the final value $u_f > 0.5$.

On the contrary, the Euler-Lagrange equations for the components of the variational parameter $\mathbf{v}$ are not trivial and read

$$\begin{aligned} i\dot{\phi}_{\mathbf{i}0} + i\frac{\partial f}{\partial \phi^*_{\mathbf{i}0}} - \frac{\partial h}{\partial \phi^*_{\mathbf{i}0}} &= 0\,, \\ i\dot{\phi}_{\mathbf{i}1} + i\frac{\partial f}{\partial \phi^*_{\mathbf{i}1}} - \frac{\partial h}{\partial \phi^*_{\mathbf{i}1}} &= 0\,, \\ i\frac{\partial f}{\partial \epsilon_{\mathbf{ij}}} - \frac{\partial h}{\partial \epsilon_{\mathbf{ij}}} - i\frac{d}{dt}\frac{\partial f}{\partial \dot{\epsilon}_{\mathbf{ij}}} &= 0\,, \end{aligned} \tag{11}$$

plus their complex conjugates. Assuming translational invariance, we can discard the site index in the above equations. The resulting differential equations are lengthy but can be written in the following matrix form

$$\hat{B}\big[\mathbf{v}(t)\big]\ \dot{\mathbf{v}}(t) = \mathbf{a}\big[\mathbf{v}(t)\big]\,, \tag{12}$$

i.e. like a set of ordinary first order non-linear differential equations, which can be numerically integrated by Runge-Kutta type of algorithms, see Supplemental Material, Sec.III [19].

In Fig. 1 we plot the long-time average of the double occupancy per site. At $u_c \simeq 0.6575$ we observe a first dynamical anomaly, which is actually the already known *dynamical transition* [8, 9, 12] at which the system shows a rapid relaxation to a Mott insulator (cf. Fig. 2a). Within Gutzwiller type of wavefunctions, the Mott transition is characterised by an order parameter $R = \phi_0\,\phi_1^* + \phi_1\,\phi_0^*$, which is finite in the metal and vanishes in the insulator [9, 20]. Formally R is defined by observing that the action of the projected operator $\mathcal{P}_i^\dagger\, c_{i\sigma}\, \mathcal{P}_i$ on the Slater determinant ψ_0 is the same as $R\, c_{i\sigma}$, so that R can be regarded as the quasiparticle component in the physical electron $c_{i\sigma}$. In Fig. 2b we show that, for $u_f < u_c$, $R(t)$ oscillates around a finite value, whereas above u_c it oscillates around zero, as clear in the inset where its time average is ploted. Therefore our improved wavefunction also points to a genuine dynamical Mott transition occurring at u_c, which, as we mentioned, contrasts the belief that the system thermalises.

In addition, we note two further dynamical anomalies at $u_f \simeq 0.77$ and $u_f = u_* \simeq 1.0326$, the latter more pronounced. To better explore their nature, in Fig. 3 we draw the frequency spectra of $R(t)$ and of the real part of $\epsilon(t)$, which show that both anomalies are actually triggered by the frequency crossing of different modes. In addition, at u_* there is also one mode that gets soft, not much different from what happens at u_c. In order to identify the origin of the different modes and the meaning of the softening, we compare the frequency spectrum of $R(t)$ with the corresponding one in the simpler time-dependent Gutzwiller wavefunction [9], see Sec.IV of the Supplemental Material [19], which lacks the spin correlations brought by the Schrieffer-Wolff transformation. Both spectra have in common the mode with frequency ω_H, see Fig. 3a. We thus conclude that ω_H originates solely from the dynamics of charge degrees of freedom, and can be associated with the *Hubbard-band mode* discussed in Ref. [21] that becomes soft at the equilibrium Mott transition. In the present non-equilibrium condition, the softening of the same mode and its higher harmonics is a further confirmation that u_c signals a genuine dynamical Mott transition.

On the other hand, the Schrieffer-Wolff transformation leads to the appearance of a new mode that does not softens at u_c, and which we associate to the spin exchange J of Eq. (9) and thus denote as exchange mode ω_J, marked with a blue dashed line in Fig. 3.

We have found that all remaining frequencies in Fig.3a

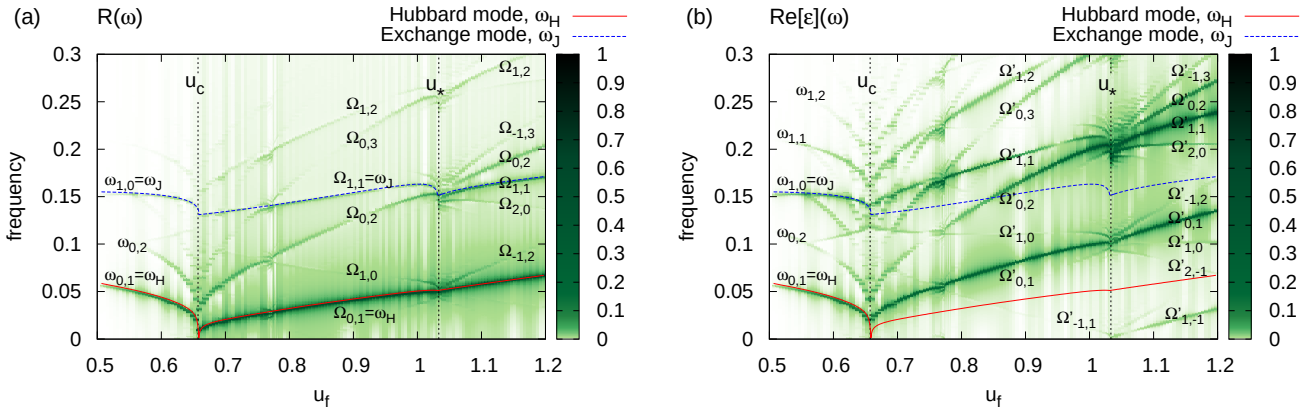

FIG. 3: Frequency spectra of $R(t)$, i.e. the real part of $\phi_0\phi_1^*$, and of the real part of ϵ, panels (a) and (b), respectively. The meaning of the frequency labels is explained in the main text.

are quantised linear combinations of the two principal frequencies ω_H and ω_J, as expected because of the nonlinear character of the Euler-Lagrange equations (11). We shall label those secondary frequencies by two integers n, k, and denote them as $\omega_{n,k}$ for $u_f < u_c$, while, above u_c, as $\Omega_{n,k}$ and $\Omega'_{n,k}$, in the power spectra of $R(t)$, Fig. 3a, and $\epsilon(t)$, Fig. 3b, respectively. These frequencies are constructed according to the following rules:

$$\begin{aligned} \omega_{n,k} &= n\,\omega_J + k\,\omega_H\,, \\ \Omega_{n,k} &= n\,(\omega_J - \omega_H) + (2k-1)\,\omega_H\,, \\ \Omega'_{n,k} &= \Omega_{n,k} + \omega_H = n\,(\omega_J - \omega_H) + 2k\,\omega_H\,. \end{aligned} \tag{13}$$

Accordingly, mode crossings occur whenever $\omega_J = (2m+1)\,\omega_H$, and thus the anomaly at $u_f \simeq 0.77$ corresponds to $m = 2$ while that at u_* to $m = 1$. Moreover, the apparent softening in the dynamics of ϵ is in reality the vanishing of the linear combination $\Omega'_{\pm1,\mp1}$. In other words, the anomaly at u_* is not characterised by the softening of any of the principal modes, ω_H or ω_J, and therefore it is not to be confused with a genuine dynamical transition. Nonetheless, close to u_* we do find changes in physical properties. In Fig. 4 we plot as function of u_f the time average $J_{\rm av}$ of the spin exchange $J(t)$ in Eq. (9), the region covered by its time fluctuations, as well as its equilibrium value $J_{\rm eq}$. We observe that, just before u_*, $J_{\rm av}$ turns from antiferromagnetic to ferromagnetic and its fluctuations grow larger, which suggests a change in character of the spin correlations. We argue it might correspond to the melting of antiferromagnetism that should occur when suddenly increasing U starting from a Néel ordered state [22].

In summary, we have studied the quench dynamics in the paramagnetic sector of the half-filled single-band Hubbard model on an infinitely coordinated Bethe-lattice, by means of a variational Gutzwiller wavefunction enriched with spin correlations by a variational Schrieffer-

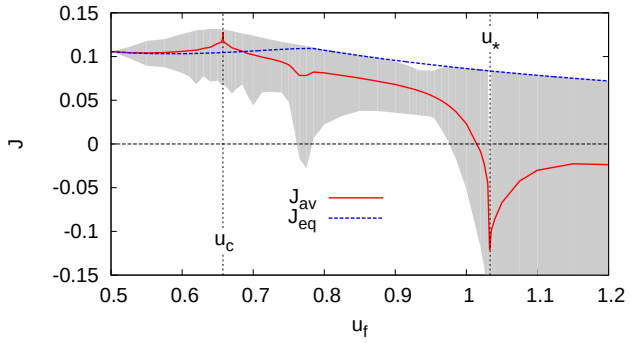

FIG. 4: Red solid line: time average value $J_{\rm av}$ of $J(t)$ in Eq. (9), as function of u_f. Blue dashed line: the value $J_{\rm eq}$ of J obtained at equilibrium by minimising the energy at $u = u_f$. In grey we indicate the region covered by the time fluctuations of $J(t)$.

Wolff transformation. We have confirmed the existence of a dynamical Mott transition at odds with the belief that the model should finally relax to a thermal state. Even though the variational wavefunction does not allow for all dissipative channels that exist in the real time evolution, we nonetheless believe that the softening of the Hubbard-band mode with frequency ω_H, which signals the Mott transition at equilibrium [21], is a genuine phenomenon that will not be swept out in more rigorous calculations. In addition we have found that the time-dependent Schrieffer-Wolff transformation yields non-trivial spin correlations that undergo a dynamical change for a final interaction value quite beyond the dynamical Mott transition.

Acknowledgements. MMW acknowledges support from the Polish Ministry of Science and Higher Education under the "Mobility Plus" programme, Agreement No. 1265/MOB/IV/2015/0, as well as from the Foundation

for Polish Science under the "START" programme. MF acknowledges support from European Union under the H2020 Framework Programme, ERC Advanced Grant No. 692670 "FIRSTORM".

* Electronic address: mwysoki@sissa.it
† Electronic address: fabrizio@sissa.it

[1] C. Giannetti, M. Capone, D. Fausti, M. Fabrizio, F. Parmigiani, and D. Mihailovic, Adv. Phys. **65**, 58 (2016), URL http://dx.doi.org/10.1080/00018732.2016.1194044.

[2] A. Cavalleri, C. Tóth, C. W. Siders, J. A. Squier, F. Ráksi, P. Forget, and J. C. Kieffer, Phys. Rev. Lett. **87**, 237401 (2001), URL https://link.aps.org/doi/10.1103/PhysRevLett.87.237401.

[3] B. Mayer, C. Schmidt, A. Grupp, J. Bühler, J. Oelmann, R. E. Marvel, R. F. Haglund, T. Oka, D. Brida, A. Leitenstorfer, et al., Phys. Rev. B **91**, 235113 (2015), URL https://link.aps.org/doi/10.1103/PhysRevB.91.235113.

[4] L. Stojchevska, I. Vaskivskyi, T. Mertelj, P. Kusar, D. Svetin, S. Brazovskii, and D. Mihailovic, Science **344**, 177 (2014), ISSN 0036-8075, URL http://science.sciencemag.org/content/344/6180/177.

[5] J. Zhang, X. Tan, M. Liu, S. W. Teitelbaum, K. W. Post, F. Jin, K. A. Nelson, D. N. Basov, W. Wu, and R. D. Averitt, Nat. Mater. **15**, 956 (2016).

[6] D. Fausti, R. I. Tobey, N. Dean, S. Kaiser, A. Dienst, M. C. Hoffmann, S. Pyon, T. Takayama, H. Takagi, and A. Cavalleri, Science **331**, 189 (2011), ISSN 0036-8075, URL http://science.sciencemag.org/content/331/6014/189.

[7] M. Mitrano, A. Cantaluppi, D. Nicoletti, S. Kaiser, A. Perucchi, S. Lupi, P. Di Pietro, D. Pontiroli, M. Ricc, S. R. Clark, et al., Nature **530**, 461 (2016).

[8] M. Eckstein, M. Kollar, and P. Werner, Phys. Rev. Lett. **103**, 056403 (2009), URL http://link.aps.org/doi/10.1103/PhysRevLett.103.056403.

[9] M. Schiró and M. Fabrizio, Phys. Rev. Lett. **105**, 076401 (2010), URL http://link.aps.org/doi/10.1103/PhysRevLett.105.076401.

[10] M. Schiró and M. Fabrizio, Phys. Rev. B **83**, 165105 (2011), URL https://link.aps.org/doi/10.1103/PhysRevB.83.165105.

[11] M. Sandri, M. Schiró, and M. Fabrizio, Phys. Rev. B **86**, 075122 (2012), URL http://link.aps.org/doi/10.1103/PhysRevB.86.075122.

[12] F. Hofmann, M. Eckstein, and M. Potthoff, Phys. Rev. B **93**, 235104 (2016), URL https://link.aps.org/doi/10.1103/PhysRevB.93.235104.

[13] S. A. Hamerla and G. S. Uhrig, Phys. Rev. B **87**, 064304 (2013), URL https://link.aps.org/doi/10.1103/PhysRevB.87.064304.

[14] S. A. Hamerla and G. S. Uhrig, Phys. Rev. B **89**, 104301 (2014), URL https://link.aps.org/doi/10.1103/PhysRevB.89.104301.

[15] M. M. Wysokiński and M. Fabrizio, Phys. Rev. B **95**, 161106(R) (2017), URL https://link.aps.org/doi/10.1103/PhysRevB.95.161106.

[16] K. A. Chao, J. Spałek, and A. M. Oleś, J. Phys. C **10**, L271 (1977).

[17] M. Eckstein, J. H. Mentink, and P. Werner (2017), arXiv:1703.03269.

[18] C. Weber, A. Amaricci, M. Capone, and P. B. Littlewood, Phys. Rev. B **86**, 115136 (2012), URL https://link.aps.org/doi/10.1103/PhysRevB.86.115136.

[19] See Supplemental Material at [URL].

[20] R. Žitko and M. Fabrizio, Phys. Rev. B **91**, 245130 (2015), URL https://link.aps.org/doi/10.1103/PhysRevB.91.245130.

[21] M. Fabrizio, Phys. Rev. B **95**, 075156 (2017), URL https://link.aps.org/doi/10.1103/PhysRevB.95.075156.

[22] M. Sandri and M. Fabrizio, Phys. Rev. B **88**, 165113 (2013), URL https://link.aps.org/doi/10.1103/PhysRevB.88.165113.

Supplemental Material to "Interplay of charge and spin dynamics after an interaction quench in the Hubbard model"

ACCURACY OF EXPANSION AT EQUILIBRIUM

In our present considerations, while expanding unitary transformed operators, we stop expansion at the third order in power of ϵ and we have taken into account all incoherent processes involving two and three neighbouring sites on the Bethe lattice. This approximation provides a satisfactory description of the paramagnetic state of the Hubbard model for $U/8T_0 \gtrsim 0.5$ when compared to the exact results of dynamical mean-field theory (DMFT) [2] (cf. Fig. 5). For the sake of completeness we have also plotted results obtained by extending our method by including also four site processes that already properly describes the system at any U [1]. The departures from the more accurate approximation for $U/8T_0 \gtrsim 0.5$ are small and only quantitative.

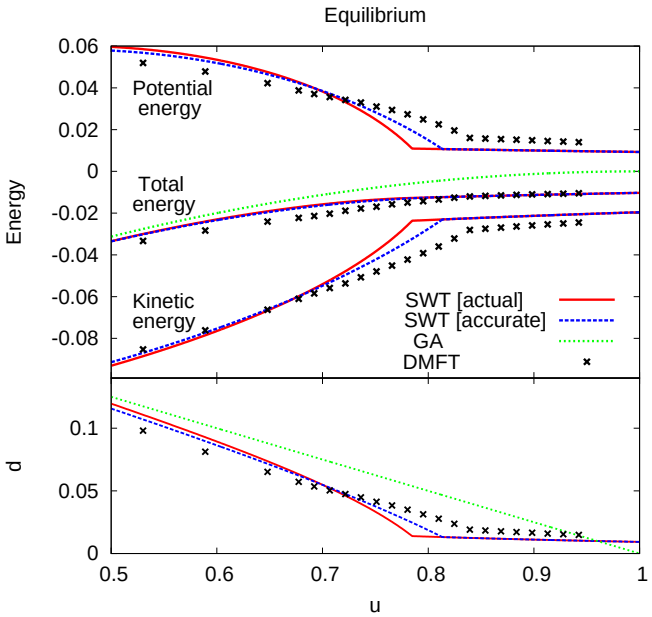

FIG. 5: Comparison between equilibrium energies and averaged double occupancies (d) between different many-body methods: SWT [actual] - present technique under actual approximation; SWT [accurate] - present technique under more accurate approximation incorporating incoherent processes involving 4 sites (used in Ref. 1); GA - Gutzwiller approximation, or 0th order expansion in power of ϵ of the present technique; DMFT - dynamical mean field theory providing numerically exact solution [2].

EXPLICIT FORM OF FUNCTIONS DETERMINING ACTION

For the sake of completeness we explicitly show how to approximate time derivative operator by taking its average with the unitary transformed Gutzwiller wavefunction,

$$\begin{aligned}\langle\psi_0|\mathcal{P}_G^\dagger U^\dagger i\frac{d}{dt}U\mathcal{P}_G|\psi_0\rangle \simeq\ & i\langle\psi_0|\dot{\psi}_0\rangle + i\langle\psi_0|\mathcal{P}_G^\dagger\dot{\mathcal{P}}_G|\psi_0\rangle \\ & + i\langle\psi_0|\mathcal{P}_G^\dagger\dot{A}\mathcal{P}_G|\psi_0\rangle - \frac{i}{2}\langle\psi_0|\mathcal{P}_G^\dagger[A,\dot{A}]\mathcal{P}_G|\psi_0\rangle \\ & + \frac{i}{6}\langle\psi_0|\mathcal{P}_G^\dagger\big[A,[A,\dot{A}]\big]\mathcal{P}_G|\psi_0\rangle,\end{aligned} \tag{14}$$

where,

$$i\langle\psi_0|\mathcal{P}_G^\dagger\dot{\mathcal{P}}_G|\psi_0\rangle = i\sum_{\mathbf{i}}(\phi_{1\mathbf{i}}^*\dot{\phi}_{1\mathbf{i}} + \phi_{0\mathbf{i}}^*\dot{\phi}_{0\mathbf{i}}). \tag{15}$$

Now we can readily provide explicit forms of functions f and h introduced in the main manuscript ($N = \sum_{\mathbf{i}} 1$),

$$\begin{aligned}\frac{f}{N} =& \frac{T_0 t}{V}(\dot{\epsilon}\phi_0^{*2}\phi_1^2 - \dot{\epsilon}^*\phi_0^2\phi_1^{*2}) - \frac{1}{4}(\dot{\epsilon}\epsilon^* - \epsilon\dot{\epsilon}^*)(|\phi_0|^4 - |\phi_1|^4) \\ & - \frac{3T_0^2}{V^2}(\dot{\epsilon}\epsilon^* - \epsilon\dot{\epsilon}^*)(|\phi_0|^2 - |\phi_1|^2)|\phi_0|^2|\phi_1|^2 \\ & + \frac{T_0}{V}(\epsilon\dot{\epsilon}^* - \dot{\epsilon}\epsilon^*)(|\phi_0|^2 + |\phi_1|^2)\left(\epsilon\phi_0^{*2}\phi_1^2 + \epsilon^*\phi_0^2\phi_1^{*2}\right),\end{aligned} \tag{16}$$

$$\begin{aligned}\frac{h}{N} =&\frac{U}{2}\phi_0\phi_0^* - T_0(\phi_0\phi_1^* + \phi_0^*\phi_1)^2 + \frac{T_0U}{V}(\epsilon\phi_0^{*2}\phi_1^2 + \epsilon^*\phi_0^2\phi_1^{*2}) + \big[\frac{V}{2}(\epsilon+\epsilon^*) - \frac{1}{2}|\epsilon|^2U\big](|\phi_0|^4 - |\phi_1|^4)\\ &+ \frac{3T_0^2}{V^2}\big[|\epsilon|^2U + (\epsilon^*+\epsilon)V\big](|\phi_0|^2 - |\phi_1|^2)|\phi_0|^2|\phi_1|^2 + \frac{3T_0^2}{V}(|\phi_0|^2 - |\phi_1|^2)\left(\epsilon\phi_0^{*2}\phi_1^2 + \epsilon^*\phi_0^2\phi_1^{*2}\right)\\ &+ \frac{T_0}{V}\Big[\frac{3V}{2}(\epsilon+\epsilon^*) - |\epsilon|^2U\Big](|\phi_0|^2 + |\phi_1|^2)\left(\epsilon\phi_0^{*2}\phi_1^2 + \epsilon^*\phi_0^2\phi_1^{*2}\right) + 3T_0|\epsilon|^2(|\phi_0|^2 + |\phi_1|^2)|\phi_0|^2|\phi_1|^2\\ &- \frac{2}{3}|\epsilon|^2V(\epsilon+\epsilon^*)(|\phi_0|^4 - |\phi_1|^4)(|\phi_0|^2 + |\phi_1|^2).\end{aligned} \tag{17}$$

MANAGING EQUATIONS FOR RUNGE-KUTTA ALGORITHM

We need to deal with a matrix ordinary differential equation in the form

$$\hat{B}[\mathbf{v}]\dot{\mathbf{v}} = \mathbf{a}(\mathbf{v}), \tag{18}$$

where $\mathbf{v} \in \{\phi_0, \phi_0^*, \phi_1, \phi_1^*, \epsilon, \epsilon^*\}$ is a vector in which we have stored all variational variables. Moreover $\hat{B}$ is 6x6 matrix and $\mathbf{a}$ is 6 component vector, both with elements functionally depending on the variables from $\mathbf{v}$. In order to efficiently proceed with numerical Runge-Kutta method we should put our equation in a following form

$$\dot{\mathbf{v}} = \hat{B}^{-1}\mathbf{a} \tag{19}$$

Because matrix $\hat{B}$ is highly complicated function of variables from vector $\mathbf{v}$ it is not particularly straightforward to calculate its inverse. For that reason it is quite convenient to first analytically reorganise equations into manageable form.

Usual Runge-Kutta algorithms demand functional form of the coefficients up to the second order expansion in powers of small time interval δt

$$\begin{aligned}\mathbf{v}_k(t+\delta t) \simeq& \mathbf{v}_k(t) + (\hat{B}^{-1}\mathbf{a})_k\delta t\\ &+ \sum_i \frac{\partial(\hat{B}^{-1}\mathbf{a})_k}{\partial\mathbf{v}_i}(\hat{B}^{-1}\mathbf{a})_i\frac{\delta t^2}{2},\end{aligned} \tag{20}$$

where subscript k (or i) denotes k-th (or i-th) element of the vector. In above we have assumed that neither $\hat{B}$ nor $\mathbf{a}$ are explicitly time-dependent as it is the case in considered situation.

Analytical forms of coefficients in expansion in (20) are generally inaccessible. For that reason in a following we provide simple and efficient numerical prescription for evaluating these coefficients at any instance of time. By using the so-called LU decomposition we may easily solve following matrix equations,

$$\begin{aligned}&\hat{B}\mathbf{x} = \mathbf{a} \quad \Rightarrow \quad \mathbf{x}_k = (\hat{B}^{-1}\mathbf{a})_k,\\ &\hat{B}\mathbf{y}^i = \frac{\partial\mathbf{a}}{\partial\mathbf{v}_i} \quad \Rightarrow \quad \mathbf{y}_k^i = (\hat{B}^{-1}\frac{\partial\mathbf{a}}{\partial\mathbf{v}_i})_k,\\ &\hat{B}\mathbf{z}^i = -\frac{\partial\hat{B}}{\partial\mathbf{v}_i}\mathbf{x} \quad \Rightarrow \quad \mathbf{z}_k^i = -(\hat{B}^{-1}\frac{\partial\hat{B}}{\partial\mathbf{v}_i}\mathbf{x})_k.\end{aligned} \tag{21}$$

Now taking advantage of the relation

$$\frac{\partial\hat{B}^{-1}}{\partial\mathbf{v}_i} = -B^{-1}\frac{\partial\hat{B}}{\partial\mathbf{v}_i}B^{-1} \tag{22}$$

we may determine

$$\begin{aligned}\frac{\partial(\hat{B}^{-1}\mathbf{a})_k}{\partial\mathbf{v}_i} &= (\frac{\partial\hat{B}^{-1}\mathbf{a}}{\partial\mathbf{v}_i})_k = (\frac{\partial\hat{B}^{-1}}{\partial\mathbf{v}_i}\mathbf{a})_k + (\hat{B}^{-1}\frac{\partial\mathbf{a}}{\partial\mathbf{v}_i})_k\\ &= -(\hat{B}^{-1}\frac{\partial\hat{B}}{\partial\mathbf{v}_i}\hat{B}^{-1}\mathbf{a})_k + \mathbf{y}_k^i\\ &= -(B^{-1}\frac{\partial\hat{B}}{\partial\mathbf{v}_i}\mathbf{x})_k + \mathbf{y}_k^i = \mathbf{z}_k^i + \mathbf{y}_k^i\end{aligned} \tag{23}$$

Finally necessary formula (20) for the Runge-Kutta algorithm can be expressed as,

$$\begin{aligned}\mathbf{v}_k(t+\delta t) \simeq& \mathbf{v}_k(t) + \delta t\,\mathbf{x}_k(t)\\ &+ \frac{\delta t^2}{2}\sum_i[\mathbf{z}_k^i(t) + \mathbf{y}_k^i(t)]\,\mathbf{x}_i(t),\end{aligned} \tag{24}$$

which together with Eqs. (21) are easily manageable numerically for arbitrary long at complicated functional forms of elements of matrix $\hat{B}$ and vector $\mathbf{a}$. The results of the main paper has been obtained with embedded 8th order Runge-Kutta Prince-Dormand method with 9th order error estimate provided within the GNU Scientific Library.

FOURIER ANALYSIS OF $R(t)$ IN tGA

Under the time-dependent Gutzwiller approximation (tGA) [3] the dynamical properties of the quenched Hubbard model at half-filling can be studied by solving following coupled differential equations,

$$\begin{aligned}i\dot{\phi}_0 &= \frac{u_f}{2}\phi_0 - \frac{1}{4}(\phi_0\phi_1^* + \phi_0^*\phi_1)\phi_1,\\ i\dot{\phi}_1 &= -\frac{1}{4}(\phi_0\phi_1^* + \phi_0^*\phi_1)\phi_0.\end{aligned} \tag{25}$$

In Fig. 6 we show a Fourier analysis of real time evolution of $R = \phi_0\phi_1^* + \phi_1\phi_0^*$.

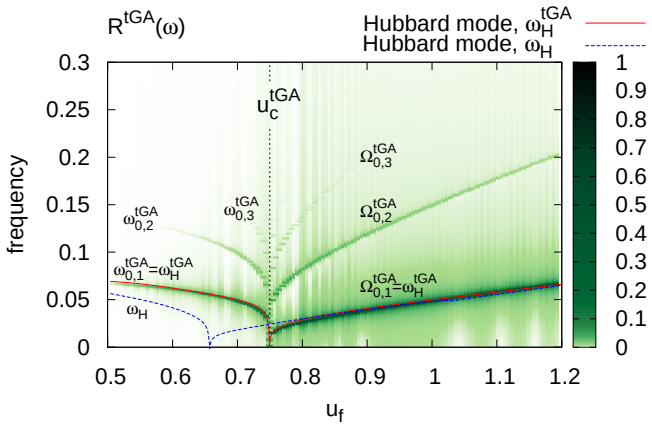

FIG. 6: Intensity (in arbitrary units) of frequencies obtained from a Fourier analysis of the long-time evolution ($t \cdot 8T_0 \in \{0, 1000\}$) of the parameter R (see main manuscript) under the time-dependent Gutzwiller approximation (tGA) [3]. The description of frequencies with two integer numbers is analogical to this from main manuscript (cf. Eq. (13,14)) under assumption that $\omega_J = 0$. For the comparison we also plot Hubbard mode resulting from the method presented in the main manuscript i.e., tGA supplemented with a variational time-dependent Schrieffer-Wolff transformation.

* Electronic address: mwysoki@sissa.it
† Electronic address: fabrizio@sissa.it

[1] M. M. Wysokiński and M. Fabrizio, Phys. Rev. B **95**, 161106(R) (2017), URL https://link.aps.org/doi/10.1103/PhysRevB.95.161106.
[2] C. Weber, A. Amaricci, M. Capone, and P. B. Littlewood, Phys. Rev. B **86**, 115136 (2012), URL https://link.aps.org/doi/10.1103/PhysRevB.86.115136.
[3] M. Schiró and M. Fabrizio, Phys. Rev. Lett. **105**, 076401 (2010), URL http://link.aps.org/doi/10.1103/PhysRevLett.105.076401.